Prog Addit Manuf (2017) 2:19–30
DOI 10.1007/s40964-017-0020-4

FULL RESEARCH ARTICLE

Optimization of selective laser sintering process parameters to achieve the maximum density and hardness in polyamide parts

Sharanjit Singh[1] · Anish Sachdeva[2] · Vishal S. Sharma[2]

Received: 8 December 2016 / Accepted: 14 March 2017 / Published online: 28 March 2017

Abstract Density and hardness of selective laser-sintered parts are influenced by the different sintering parameters. The selection of sintering parameters plays a vital role to achieve the high precision of end use functional parts. These parts are widely used in the industries such as automobile, aerospace, and for medical applications [Sustarsic et al. (Mater Manuf Process 24:837–841, 2009), Shah et al. (Mater Manuf Process 25:1372–1380, 2010)]. In this study, laser power, scan spacing, bed temperature, hatch length, and scan count were the parameters taken into account for experimentation. Face-centered central composite design was used as a statistical design of experiment technique to set the optimal laser sintering parameters. A relationship between these parameters had also been developed with the generation of different mathematical models. The adequacies of these models were confirmed using analysis of variance. The study concluded that laser power, scan spacing, bed temperature, and hatch length have higher influence on density and hardness of polyamide laser-sintered parts. Among these parameters, scan spacing is the most significant parameter for both density and hardness measures. Laser power—24.05 mm, scan spacing—0.1 mm, bed temperature—173.65 °C, hatch length—114.64 mm, and scan count—2 are the optimum levels to maximize the density and hardness.

Keywords Selective laser sintering · Hardness · Density

1 Introduction

Selective laser sintering (SLS) is a rapid manufacturing process which uses powder material for fabrication of different parts directly from CAD drawing. Different common engineering thermoplastics such as polyamides, ABS, polycarbonate, and nylons, and for metal parts the materials such as titanium, stainless steel, and tool steel are broadly used for fabrication of parts [3]. Laser sintering of plastic and metallic parts is very challenging job mainly due to their weak strength, dimensional inaccuracy, and poor surface roughness [4]. Density and hardness are two key output parameters that affect the quality of produced parts, and highly depend upon the level of laser sintering. Along with other mechanical properties, in the case of polymeric materials, there is direct relationship between hardness and density of parts [5]. Hardness discusses the homogeneity of the polymeric parts, which is related to the compaction condition and density of part [6]. Therefore, it becomes necessary to take extra care while choosing the different laser sintering parameters. This can be only possible with the experience of operator, available guidelines, and with the help of previous research work. In laser sintering, the level of parameters varies according to the materials used. This is the major problem to deal with, which also limits/diminishes the scope and applications of these laser-sintered parts.

✉ Sharanjit Singh
malhi.sharanjit@gmail.com

Anish Sachdeva
asachdeva@nitj.ac.in

Vishal S. Sharma
sharmavs@nitj.ac.in

[1] Department of Mechanical Engineering, DAV University , Jalandhar, Punjab 144012, India

[2] Department of Industrial and Production Engineering, Dr B R Ambedkar National Institute of Technology, Jalandhar, Punjab 144011, India

In previous years, a number of studies have been carried out using different combination of input sintering parameters to achieve the precise quality (accuracy, mechanical properties [7], and surface roughness [8] of parts [9]). But, there is still a scope to fabricate high-quality parts having wide engineering as well as other applications. Our scrutiny of the literature evidences that there were few reports in which density was studied using polymers as a work material. Gibson and Shi [10] investigated the influence of different laser-sintered parameters with the use of nylon powder. It is found that density increases at higher values of laser power, but decreases with the increase in the value of scan spacing and scan speed. Williams and Deckard [11] also investigated the influence of laser-sintered parameters on polycarbonate-made parts and concluded that the delay time and spot size have significant influence on the strength and density of produced parts. Ho et al. [12] studied the physical density, tensile properties, and morphology of polycarbonate-made specimens. It is found that the physical density and tensile properties increase with the increase in energy density. Tontowi and Childs [13] examined the effect of bed temperature on part density. From this study, it is proposed that a linear relationship is required between bed temperature and energy density to achieve the maximum part density. Shi et al. [14] investigated the effect of different properties for the polymeric materials such as particle size, crystallization rate, molten viscosity, and molecular weight on the quality of SLS parts. It is further presented that by maintaining the particle size of 75–100 µm, the parts having higher density can be generated. Bugeda et al. [15] developed a model for prediction of density of SLS-made parts. Further, Vijayaraghavan et al. [16] also presented a coupled FEA–EA model for simulation of SLS-made parts for density measures.

This study seeks to experimentally characterize the density and hardness of laser-sintered polyamide parts using

Table 1 Process parameters and their values used in SLS

Variable		Fixed	
Parameters	Values	Parameters	Values
Laser power (A)	24, 28, 32 W	Scan speed	5000 mm/s
Scan spacing (B)	0.1, 0.2, 0.3 mm	Layer thickness	0.1 mm
Bed temp. (C)	172, 175, 178 °C	Roller speed	254 mm/s
Hatch length (D)	40, 100, 120 mm	Spot size	0.05 mm
Scan count (E)	1–2	Sinter scan	Off
		Beam offset	0.25 mm

Table 2 Features of hardness tester used for the experiment

S. no	Parameters	Values
1	Model	RAS
2	Max. test height (mm)	230
3	Depth of throat (mm)	133
4	Max depth of screw below base (mm)	240
5	Initial load (kgf)	10
6	Test load (kgf)	60
7	Intender	¼ steel ball
8	Scale	Rockwell number-L (HRL)
Dimension of machine		
1	Size of base (app)	430 × 170 mm
2	Height	655 mm (approx.)
3	Net weight	65 kg (approx.)

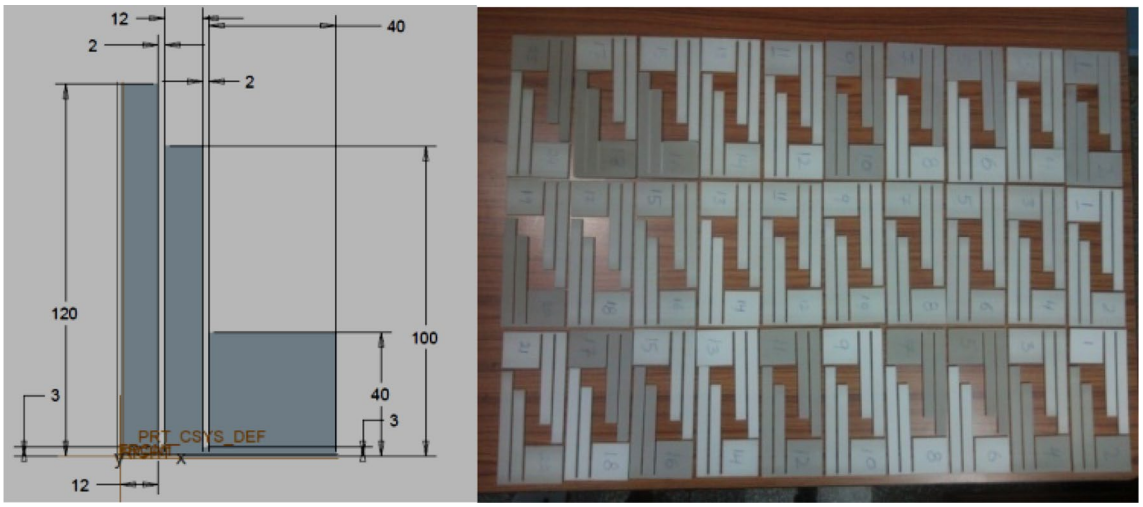

Fig. 1 Design of specimen with dimensions, specimens used for testing [8]

Table 3 Experimental design matrix and collected data

S. no	Coded values					Actual values					Density (g/cc)	Hardness (HRL)
	X_1	X_2	X_3	X_4	X_5	Laser power (W)	Scan spacing (mm)	Bed temp (°C)	Hatch length (mm)	Scan count		
1	1	1	1	1	1	32	0.3	178	120	1	0.975978	96.5
2	0	0	−1	0	1	28	0.2	172	80	1	0.952021	98
3	1	1	1	−1	1	32	0.3	178	40	1	0.961878	89.5
4	1	1	−1	−1	2	32	0.3	172	40	2	0.978337	91
5	0	0	0	0	2	28	0.2	175	80	2	1.00823	88.5
6	−1	−1	−1	−1	1	24	0.1	172	40	1	1.013525	97.5
7	0	0	0	0	2	28	0.2	175	80	2	1.00822	86.5
8	1	−1	−1	1	1	32	0.1	172	120	1	1.023454	87.5
9	−1	−1	−1	1	1	24	0.1	172	120	1	1.017932	82
10	0	0	1	0	2	28	0.2	178	80	2	0.995642	96.5
11	−1	1	−1	−1	1	24	0.3	172	40	1	0.981304	45.5
12	1	−1	−1	−1	2	32	0.1	172	40	2	1.028558	98.5
13	0	1	0	0	2	28	0.3	175	80	2	0.97012	43
14	−1	1	1	−1	2	24	0.3	178	40	2	0.964793	25
15	0	−1	0	0	2	28	0.1	175	80	2	1.0089	97.5
16	0	0	0	0	2	28	0.2	175	80	2	1.00822	93
17	0	0	0	0	1	28	0.2	175	80	1	1.00821	87
18	−1	1	−1	−1	2	24	0.3	172	40	2	0.989566	95
19	1	−1	1	1	1	32	0.1	178	120	1	0.99983	92
20	−1	1	−1	1	1	24	0.3	172	120	1	0.993627	29
21	1	1	−1	1	1	32	0.3	172	120	1	0.971315	66
22	0	0	−1	0	2	28	0.2	172	80	2	0.973161	94
23	1	1	−1	1	2	32	0.3	172	120	2	0.988803	98
24	−1	1	−1	1	2	24	0.3	172	120	2	0.998147	61
25	−1	0	0	0	2	24	0.2	175	80	2	1.00112	77.2
26	0	0	0	−1	1	28	0.2	175	40	1	1.00824	81
27	0	0	0	0	1	28	0.2	175	80	1	1.00821	86
28	0	0	0	0	1	28	0.2	175	80	1	1.0081	90.5
29	1	−1	−1	1	2	32	0.1	172	120	2	1.027518	98
30	−1	−1	−1	−1	2	24	0.1	172	40	2	1.019525	82.5
31	−1	−1	1	1	2	24	0.1	178	120	2	1.030056	84
32	0	0	0	0	2	28	0.2	175	80	2	1.00821	86
33	−1	−1	1	1	1	24	0.1	178	120	1	0.987276	94
34	−1	−1	−1	1	2	24	0.1	172	120	2	1.014789	98.5
35	1	−1	−1	−1	1	32	0.1	172	40	1	1.018774	89.5
36	−1	−1	1	−1	1	24	0.1	178	40	1	1.007321	92
37	0	0	0	−1	2	28	0.2	175	40	2	1.00824	84
38	0	−1	0	0	1	28	0.1	175	80	1	0.99872	98.5
39	0	0	0	0	2	28	0.2	175	80	2	1.00821	82
40	−1	1	1	1	2	24	0.3	178	120	2	0.967313	75
41	−1	1	1	1	1	24	0.3	178	120	1	0.969256	78
42	1	0	0	0	1	32	0.2	175	80	1	0.99212	87
43	0	0	0	0	1	28	0.2	175	80	1	1.0082	83
44	0	0	0	0	1	28	0.2	175	80	1	1.0082	85.5
45	−1	0	0	0	1	24	0.2	175	80	1	0.99882	87
46	0	1	0	0	1	28	0.3	175	80	1	0.99833	62.5
47	1	−1	1	−1	2	32	0.1	178	40	2	1.0259	95.5

Table 3 (continued)

S. no	Coded values					Actual values					Density (g/cc)	Hardness (HRL)
	X_1	X_2	X_3	X_4	X_5	Laser power (W)	Scan spacing (mm)	Bed temp (°C)	Hatch length (mm)	Scan count		
48	1	0	0	0	2	32	0.2	175	80	2	1.0092	90.5
49	1	1	1	1	2	32	0.3	178	120	2	0.989276	69
50	1	1	1	−1	2	32	0.3	178	40	2	1.025822	89.5
51	1	−1	1	−1	1	32	0.1	178	40	1	1.030056	79.5
52	0	0	0	1	2	28	0.2	175	120	2	1.00823	84.5
53	0	0	0	0	2	28	0.2	175	80	2	1.0083	86
54	−1	1	1	−1	1	24	0.3	178	40	1	0.937157	21
55	1	−1	1	1	2	32	0.1	178	120	2	1.01499	29.5
56	0	0	0	1	1	28	0.2	175	120	1	1.0082	89
57	0	0	0	0	1	28	0.2	175	80	1	0.98218	90
58	0	0	1	0	1	28	0.2	178	80	1	0.993642	86.5
59	1	1	−1	−1	1	32	0.3	172	40	1	0.970973	84.5
60	−1	−1	1	−1	2	24	0.1	178	40	2	1.025822	34

Table 4 ANOVA for analysis of variance and adequacy of the quadratic model for density

Source	Sum of squares	*df*	Mean square	*F* Value	Prob > *F*	
Model	0.017	8	0.002	11.959	0.0001	Significant
A	0.0003	1	0.0003	2.135	0.150	
B	0.012	1	0.012	69.991	0.0001	
C	9.77E-05	1	9.77E-05	0.564	0.456	
D	2.67E-06	1	2.67E-06	0.015	0.902	
E	0.001	1	0.001	7.556	0.008	
C^2	0.001	1	0.001	10.98	0.002	
D^2	0.001	1	0.001	6.702	0.013	
AC	0.001	1	0.0007	4.353	0.042	
Residual	0.009	51	0.0001			
Lack of fit	0.008	41	0.0002	3.583	0.018	Significant
Pure error	0.001	10	5.64E-05			
Cor total	0.025	59				
Std. dev. 0.013				*R* squared 0.652		
Mean 0.999				Adj *R* squared 0.598		
C.V. 1.318				Pred *R* squared 0.502		
PRESS 0.0127				Adeq precision 12.301		

A laser power, *B* scan spacing, *C* bed temp., *D* hatch length, *E* scan count

laser power, scan spacing, bed temperature, hatch length, and scan count as a function of input parameters.

2 Experimental study

2.1 Process parameters and workpiece material

The range of the different laser-sintered parameters and the other constant parameters selected [8] for this experimental work are shown in Table 1. These parameters and their range have been selected according to the machine specifications and raw materials used. In laser sintering, the powder is preheated just below its melting temperature to facilitate sintering. The temperature in the part bed is uniformly distributed and maintained by different part heaters provided in part bed chamber. Then, appropriate parameters are applied to achieve the maximum density and hardness. Different specimens (Fig. 1) used for density and hardness testing are fabricated using SLS machine manufactured by

Table 5 ANOVA for analysis of variance and adequacy of the 2FI model for hardness

Source	Sum of squares	*df*	Mean square	*F* value	Prob > F	
Model	10664.79	8	1333.10	5.44	<0.0001	Significant
A	2070.25	1	2070.25	8.44	0.0054	
B	2695.34	1	2695.34	10.99	0.0017	
C	793.36	1	793.36	3.24	0.0780	
D	37.01	1	37.01	0.15	0.6993	
E	8.07	1	8.07	0.03	0.8568	
AB	1937.53	1	1937.53	7.90	0.0070	
AD	1128.13	1	1128.13	4.60	0.0367	
CE	1995.11	1	1995.11	8.14	0.0063	
Residual	12505.69	51	245.21			
Lack of fit	12399.69	41	302.43	28.53	<0.0001	Significant
Pure error	106.00	10	10.60			
Cor total	23170.48	59				
Std. dev. 15.66				*R* squared 0.460		
Mean 80.82				Adj *R* squared 0.376		
C.V. 19.38				Pred *R* squared 0.153		
PRESS 19615.14				Adeq precision 11.715		

A laser power, *B* scan spacing, *C* bed temp., *D* hatch length, *E* scan count

3D systems (Vanguard HS) and using duraform polyamide (3D systems) as a workpiece material. This polyamide powder is semicrystalline in nature. Aging state of powder differs, as the powder goes under heating cycle and mechanical load which results in change in mechanical properties [17]. So for experimentation mixture of 30% fresh and 70% previously used but unsintered powder is used for building parts, more amount of virgin powder cause curling and warpage.

2.2 Performance measures

Density determinations are frequently performed using Mettler Toledo AL204 balance by means of Archimedes' principle (buoyancy method) [18, 19] at room temperature with the use of *n*-Butyl acetate (0.88) as a liquid medium, which is also the method used by the density determination kit for balances. Hardness testing of different polyamide samples on top of surface is performed on Rockwell hardness tester, and the specification and other parameters are listed in Table 2. For SEM analysis, HITACHI TM3000 machine is used, and samples are prepared by coating thin layer of gold on a small piece of sample and then SEM images are captured for analysis.

2.3 Response surface methodology

Modeling and optimization of a process are important issues in manufacturing. Response surface methodology (RSM) is a statistical technique that is used in this study. RSM is commonly used to inspect and optimize the effect of two or more factors on quality criteria [20, 21]. Optimization of different parameters not only enhances the efficiency of technologist, but also develops part superiority. Since SLS is normally a multivariate problem, RSM is fitted to be an appropriate method for improving, analyzing, and optimizing the structures over feasible domain of parameter settings for density and hardness. The optimum situation has been generated by solving the regression Eqs. (1, 2) and by checking response surface contours.

Table 6 Different model generated for density and hardness

Density (scan count 1)	$-53.42265 - 0.070027\mathrm{A} - 0.18360\mathrm{B} + 0.63458\mathrm{C} - 1.30558 \times 10^{-3}\mathrm{D} - 1.84703 \times 10^{-3}\mathrm{B}^2 + 8.11732 \times 10^{-6}\mathrm{D}^2 + 4.04737 \times 10^{-4}\mathrm{AC}$
Density (scan count 2)	$-53.41330 - 0.070027\mathrm{A} - 0.18360\mathrm{B} + 0.63458\mathrm{C} - 1.30558 \times 10^{-3}\mathrm{D} - 1.84703 \times 10^{-3}\mathrm{B}^2 + 8.11732 \times 10^{-6}\mathrm{D}^2 + 4.04737 \times 10^{-4}\mathrm{AC}$
Hardness (scan count 1)	$-91.22639 + 0.97396A - 631.21528B + 0.91667C + 1.06441D + 19.45313AB - 0.037109AD$
Hardness (scan count 2)	$776.55880 + 0.97396A - 631.21528B - 4.04630C + 1.06441D + 19.45313AB - 0.037109AD$

A laser power, *B* scan spacing, *C* bed temp., *D* hatch length, *E* scan count

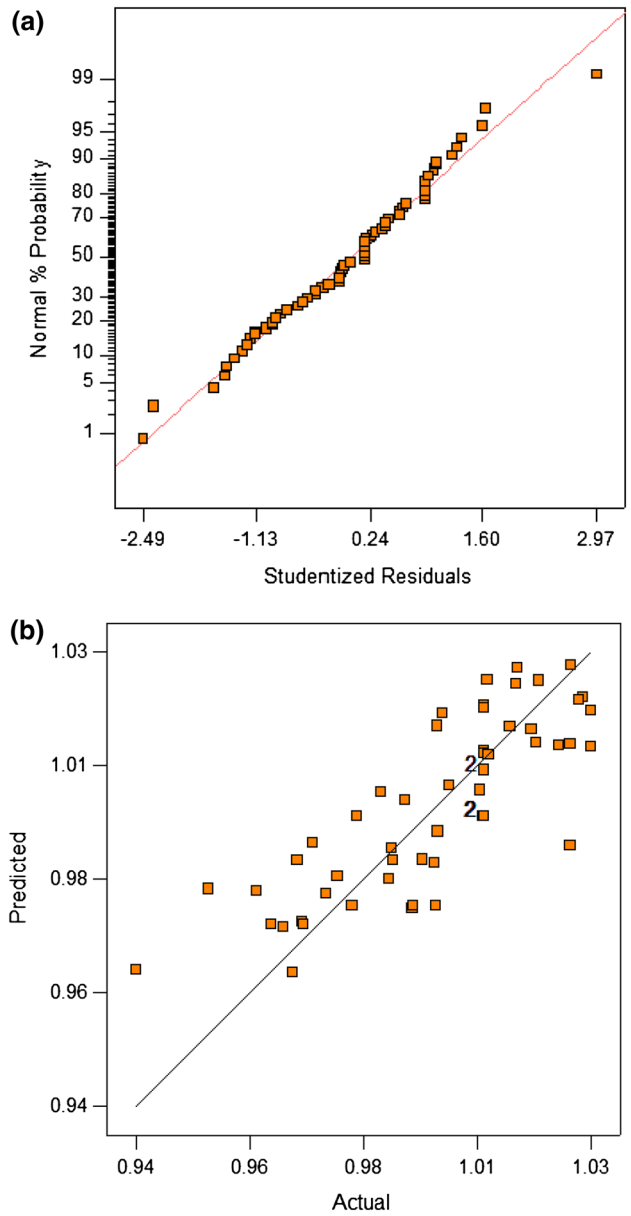

Fig. 2 **a** Normal probability plot of residuals for density. **b** Plot of predicted vs. actual response for density

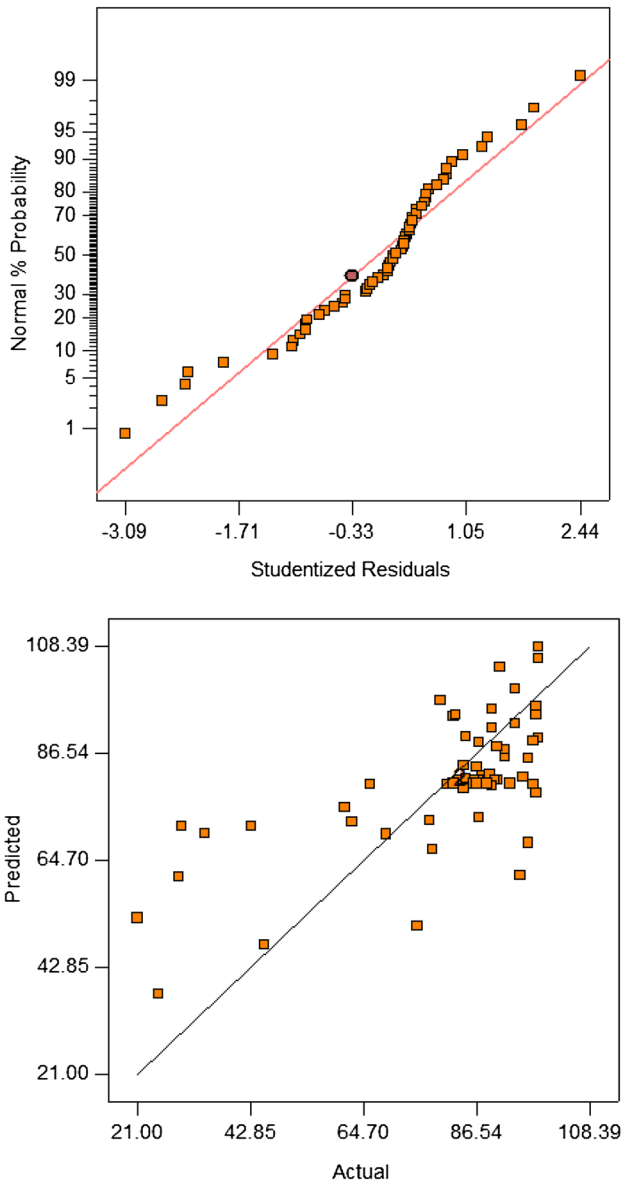

Fig. 3 **a** Normal probability plot of residuals for hardness. **b** Plot of predicted vs. actual response for hardness

$$Y = \beta_0 + \sum_{j=1}^{k} \beta_j X_j + \sum \sum_{i<j} \beta_{ij} X_i X_j + e_i \quad (1)$$

$$Y = \beta_0 + \sum_{j=1}^{k} \beta_j X_j + \sum_{j=1}^{k} \beta_{jj} X_j^2 + \sum_{i} \sum_{<j=1}^{k} \beta_{ij} X_i X_j + e_i \quad (2)$$

As there are only three levels for each factor, the appropriate model is the quadratic model, Eq. (2). Equation (2) is more appropriate because it provides protection for curvature generated from second-order effects and independently estimates the generated errors [20]. In this, Y is the response; X_i and X_j are two variables; β_0 is a constant coefficient; β_j, β_{jj}, and β_{ij} are the interaction coefficients of linear, quadratic, and second-order terms; k is the number of studied factors; and e_i is the error. The quality of the fit of this model was expressed by the value of correlation coefficient (R^2). The main indicators representing the significance and adequacy of the developed model consist of the model F value, probability value, and adequate precision.

2.4 Experimental design

In this experimental test plan, face-centered central composite design (CCD) of response surface methodology had

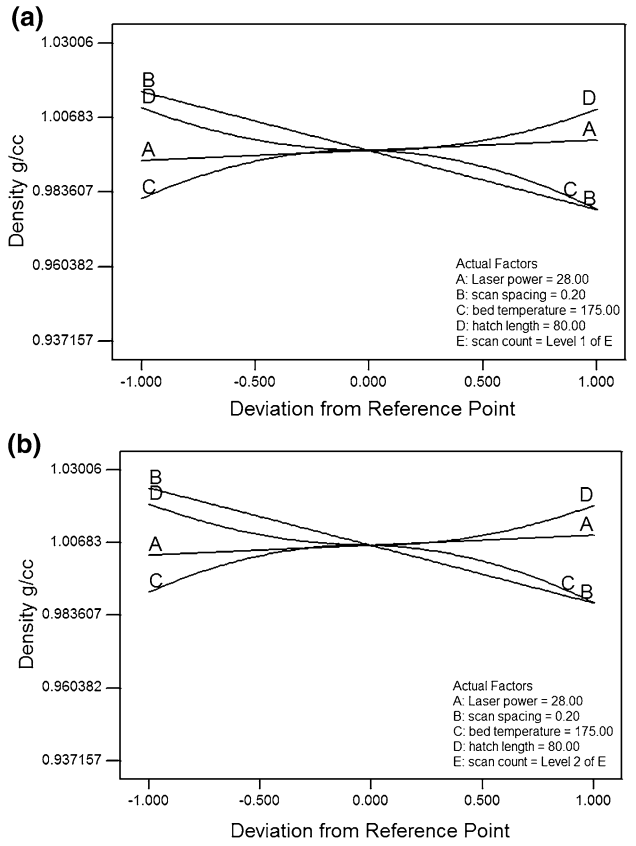

Fig. 4 Perturbation plot for density **a** at scan count 1, **b** at scan count 2

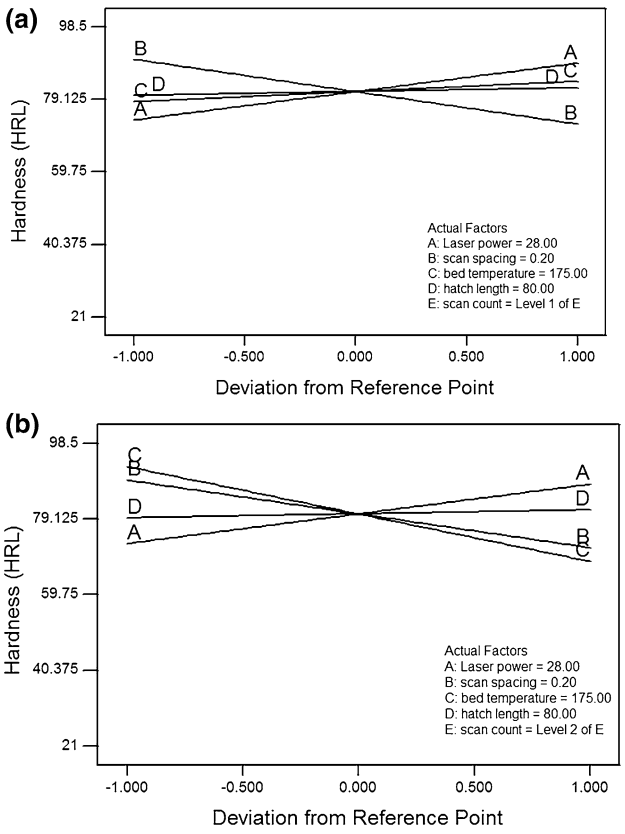

Fig. 5 Perturbation plot for hardness **a** at scan count 1, **b** at scan count 2

been used. This design provides perfect platform for generating a response surfaces. In face center CCD, the star or axial points are located on the every face or corner of the cube. This design is non-rotatable design with a value of $\alpha = 1$. A total of 60 experiments were performed at four independent input variables and one category factor. The design factors selected for study are summarized in Table 3.

3 Result and discussion

3.1 Analysis of variance

The ANOVA test is performed to verify the significance of selected parameters in the designed experimental study. The ANOVA results for both density and hardness are presented in Tables 4 and 5, respectively.

For density measures, reduced quadratic model is used as it fits the data appropriately. As shown in Table 4, model F value of 11.96 and small probability value (Prob $> F <$ 0.0500) show that the model is significant for density. The model terms having values >0.1000 are insignificant model terms [20]. The lack of fit is statistically significant as the probability values are less than 0.05. This may be due to the exact replication of the values of the independent variables in the model that provide an estimation of pure error. The predicted R^2 of 0.5018 is in reasonable agreement with the adjusted R^2 of 0.5977. The adequate precision ratio of the model is 12.302 (Adequate precision > 4), which is an adequate signal for the model [20].

Further for hardness measures, reduced 2-factor interaction (2FI) model is used as it fits the data appropriately. As shown in Table 5, model F value of 5.44 and low probability value (Prob $> F <$ 0.0500) indicate that model is significant for hardness. In case of hardness, significant lack of fit shows that there may be some systematic deviation unaccounted for in the model. Again this may due to the exact replication of the values of the independent variables in the model that provides an estimation of pure error. The predicted R^2 of 0.1534 is in reasonable agreement with the adjusted R^2 of 0.3756. The adequate precision ratio of the model is 11.715 (Adequate precision > 4), which is an adequate signal for the model developed for hardness [20].

The lower value of R square obtained in both models is undesirable, which indicates the data are scattered around the regression line. But the interpretation of variables

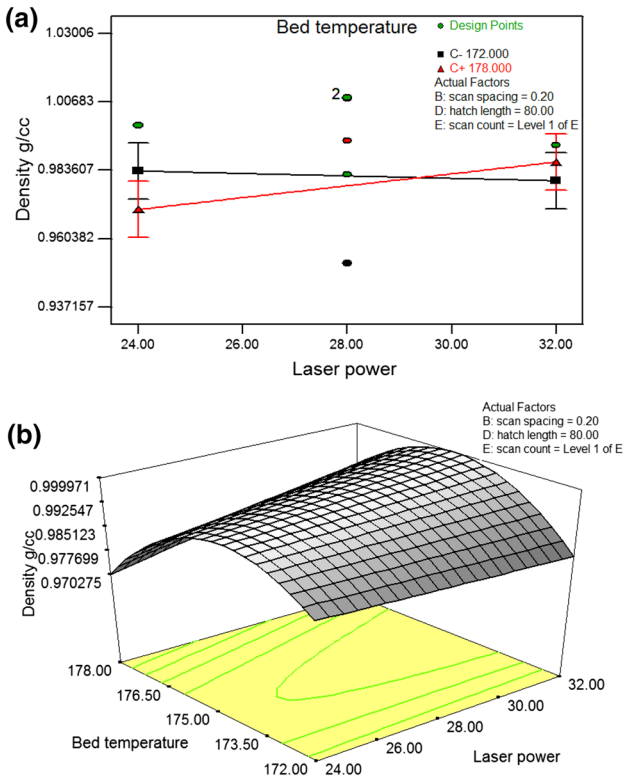

Fig. 6 Interaction and 3D response surface plots for Density. **a** Interaction between bed temperature and laser power, **b** 3D response surface plot between bed temperature and laser power

cannot be effected by the value of *R* square, if the selected parameters and generated models are significant [22].

3.2 Model formulation

The models obtained for density contained B, E, C^2, D^2, and AC as significant model terms and for hardness A, B, AB, AD, and CE are significant terms. Insignificant model terms, which have limited influence, are excluded from the study to improve the model. In terms of actual factors, an empirical relationship between performance measures and process variables can be expressed by the following equations as shown in Table 6.

To check the ability and adequacy of the generated models related to the real system, normal probability plots of the studentized residuals and the predicted data vs actual data value plot have been analyzed. Figures 2a and 3a show the normal probability plots for density and hardness, respectively. In these plots, it is seen that the residuals are falling in the straight line in both cases, which seems that the errors are normally distributed. In Figs. 2b and 3b, the predicted values of density and hardness which are generated from the obtained models and the experimental data values are equally randomly distributed.

3.3 Effect of process parameters on density and hardness

Figures 4 and 5 show the perturbation graphs for density and hardness at scan counts 1 and 2, respectively. From perturbation graphs, as shown in all figures, it can be seen that the density and hardness increase with the increase in laser power. While the increase in laser power results more heat to penetrate into the machine bed, the tendency of powder particles to get closely packed also increases. This leads toward complex structured parts having higher density and hardness. Similar trend/results are also obtained for laser power by Gibson and Shi [10] while measuring the density of polymer (Nylon)-based SLS samples. Further decrease in density and hardness is observed with increase in scan spacing. This is because the increase in scan spacing results in poor packing of the particles in the powder bed or unsintered particles. It should not be larger than the laser beam diameter. So higher scan spacing gives poor density and hardness. Gibson and Shi [10] also found similar downward trend in case of scan spacing while investigating the density of polymer-made samples. In case of bed temperature, it is noted that first density increases when bed temperature increases from 172 to 175 °C similar as investigated by Tontowi and Childs [13], but this trend reversed with the further increase in bed temperature for 175–178 °C. But for hardness as shown in Fig. 5a, it is noted that hardness increases with increase in bed temperature when scan count is 1 and this trend totally reversed with scan count is 2 (Fig. 5b), i.e., hardness lowers with increase in bed temperature. Higher bed temperature results the proper sintering of powder particles, which gives high density and hardness of sintered parts. But in case the increase in bed temperature (175–178 °C for density and at scan count 2 for hardness) leads to decrease in density and hardness confirmed that this reduction is due to polymer degradation as suggested by Ho et al. [12]. Hatch length also shows a significant effect on density and hardness. It is found that density first decreases up to middle level and then it increases with the increase in hatch length. But hardness increases continuously with the increase in hatch length. Scan count only shows the effect on density; it can be seen that density increases with increase in scan count due to proper sintering of powder particles.

3.4 Interaction effect of process parameters on density and hardness

Interaction and 3D response surface plots show the combined effect of two different variables on the selected output parameters. Figure 6a, b shows the interaction graph and 3D response surface plot of laser power and bed temperature for density measures. It can be seen that with the

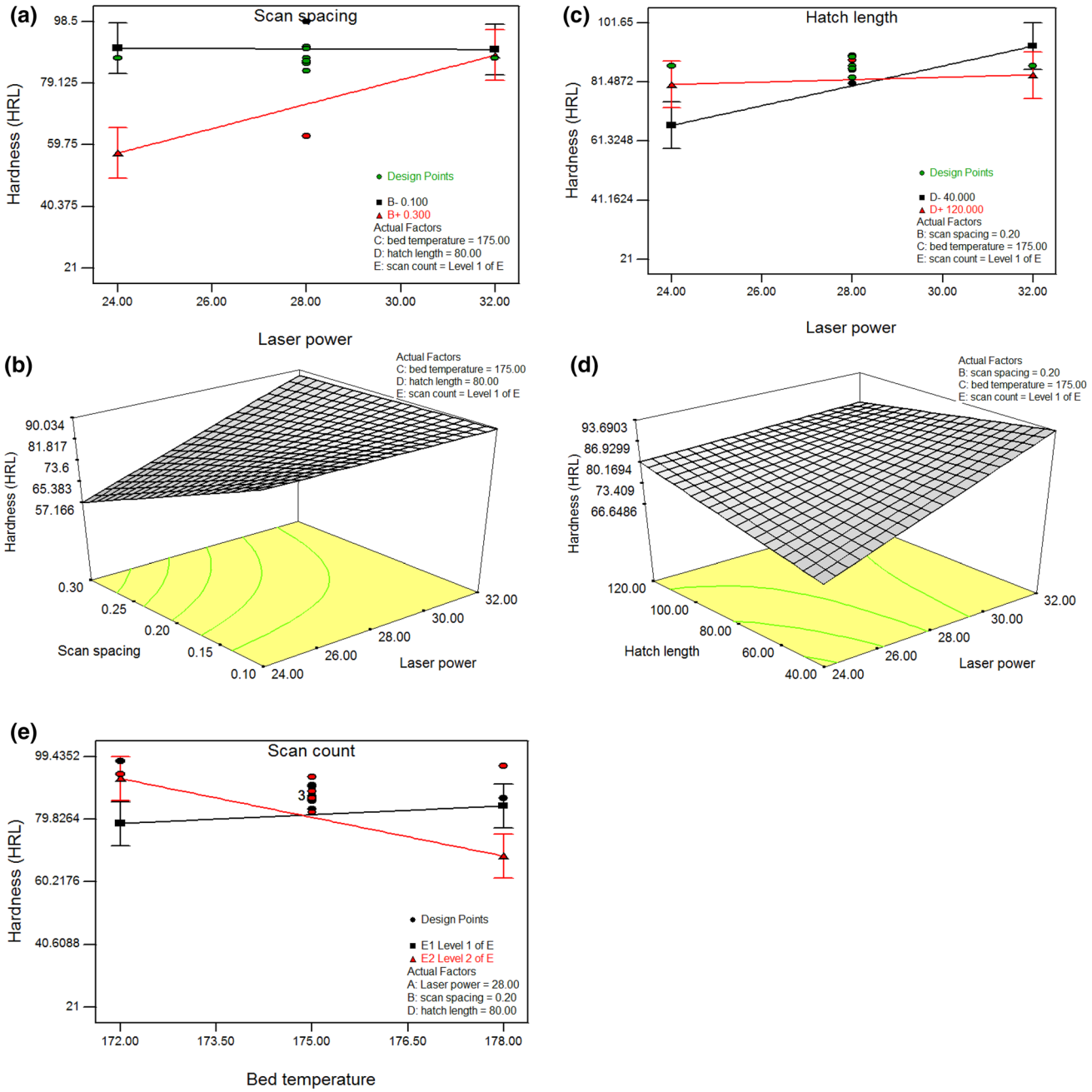

Fig. 7 Interaction and 3D response surface plots for hardness. **a** Interaction graph between laser power and scan spacing, **b** 3D response surface plot between laser power and scan spacing, **c** interaction graph between laser power and hatch length, **d** 3D response surface plot between laser power and hatch length, **e** interaction graph between bed temperature and scan count

increase in laser power from low level toward higher level the density also increases. But with the increase in the level of bed temperature, a little decrease in the value of density has been observed. Figure 7a, b demonstrates the interaction and 3D response surface plot between laser power and scan spacing for hardness measures. The specimen sintered at high level of laser power (32 W) and at low level of scan spacing (0.1 mm) exerts maximum hardness. The interaction and 3D plots between laser power and hatch length for hardness measures has been presented in Fig. 7c, d. From these graphs, it has been observed that with the increase in the level of laser power and hatch length from low level toward higher level, the hardness of fabricated specimens also increases. Figure 7e only shows the interaction graph between bed temperature and scan count for hardness measures. The higher hardness of specimen has

Table 7 Optimization results for maximizing density and hardness

S. no.	Laser power (w)	Scan spacing (mm)	Bed temperature (°C)	Hatch length (mm)	Scan count	Density (g/cc)	Hardness (HRL)	Desirability	
1	24.05	0.10	173.65	114.64	2	1.03	100.64	1	Selected
2	25.17	0.10	173.67	119.33	2	1.03	99.51	1	
3	27.24	0.10	173.06	119.85	2	1.03	99.12	1	
4	27.52	0.10	173.04	118.86	2	1.03	98.64	1	
5	25.59	0.10	173.60	114.18	2	1.03	98.8	1	
6	26.85	0.10	173.15	119.67	2	1.03	98.84	1	
7	31.76	0.11	173.28	40.28	2	1.03	100.23	1	
8	25.42	0.10	173.53	107.38	2	1.02	98.5	0.980613	
9	32.00	0.10	175.73	41.82	1	1.03	95.0	0.977223	
10	32.00	0.10	173.71	57.35	2	1.02	96.92	0.975348	

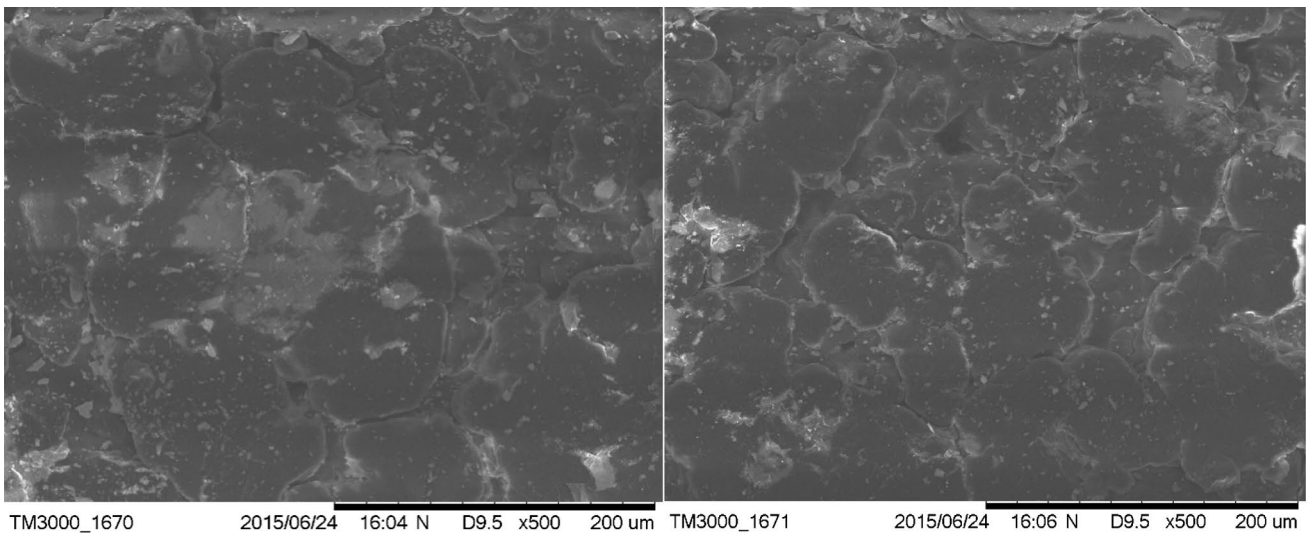

Fig. 8 Micrographs of the SLS-made specimen

been observed at higher lever of bed temperature and at low level of scan count.

3.5 Optimization and confirmation test

Optimization was carried out to determine the optimum values of input parameters to fulfill the desired goal by maximizing the density and hardness of SLS-made polyamide parts. To find the optimal condition in design space, all input parameters were set within range and performance measures at maximum to achieve desired performance. Present optimized practice combines the individual desirability's into a single number and then investigates to maximize these functions. The generated set of optimal conditions with maximum desirability function is shown in Table 7. After development of optimal level for these parameters, the next step is to confirm and verify the perfection of the performance characteristics using this optimal level of the laser-sintered parameters. An additional experiment was then performed to verify the optimum results. The values of density 1.02 g/cc and hardness 100.54 HRL were obtained from the confirmation test which agrees well with the predicted response value. Figure 8 shows the micrographs for the above specimen, it is seen that there are some gaps, otherwise the particle are properly packed due to necking process which fills the maximum pores by proper sintering/melting the powder particles.

4 Conclusion

In this study, the experiments were carried out to determine the density and hardness and to sense the effect of different process parameters on laser-sintered polyamide parts. The RSM approach was used to check the optimal working conditions, and ANOVA was also carried out to determine the significance of each process parameter on the density and hardness. The following conclusions were evolved after the study.

- The process parameter for achieving the maximum density and hardness can be obtained from the generated mathematical model. The conformation result for the generated model comes within the range.
- The scan spacing seems to be the most significant parameter for both density and hardness. The experimental results show that the increase in scan spacing results in the decrease of density and hardness as well. So to maximize these performance measures, scan spacing should be selected at a low level, i.e., 0.1 mm.
- Laser power also shows the effect on density and hardness where both increase with increase in the level of laser power.
- With increase in bed temperature, hardness continuously increases, but density first increases with an increase in bed temperature and then decreases with further increase in bed temperature.
- In case of hatch length, hardness increases with increase in the level of hatch length, while density first decreases with an increase in hatch length up to middle level and then increases with further increase in the level of hatch length.
- With increase in scan count, density also increases, but in case of hardness it only shows combined effect with bed temperature, i.e., at lower level of scan count, the increase in bed temperature leads toward the increase in hardness. But this trend totally reversed with scan count 2, i.e., hardness decreases with increase in bed temperature.
- Laser power is at 24.05 mm, scan spacing is at 0.1 mm, bed temperature is at 173.65 °C, hatch length is at 114.64 mm, and scan count is at 2 while determining the optimum level to maximize the density and hardness.

Acknowledgements The authors acknowledge the Ministry of Human Resource and Development (MHRD), Govt. of India for the financial support and Rapid Prototyping Center, Center Tool Room Ludhiana, Punjab, India for providing the SLS setup for experimentation.

References

1. Sustarsic B, Dolinsek S, Jenko M, Leskovsek V (2009) Microstructure and mechanical characteristics of DMLS tool-inserts. Mater Manuf Process 24(7–8):837–841
2. Shah K, Pinkerton AJ, Salman A, Li L (2010) Effects of melt pool variables and process parameters in laser direct metal deposition of aerospace alloys. Mater Manuf Process 25(12):1372–1380
3. Gibson I, Rosen DW, Stucker B (2010) Additive manufacturing technologies. In: Rapid Prototyping to Direct Digital Manufacturing. Springer, New York
4. Chua CK, Leong KF, Lim CS (2010) Rapid prototyping: principles and applications, 4th edn. World Scientific, Singapore
5. Crawford R (1986) Solid phase compaction of polymeric powders. Developments in Plastics Technology—3. Elsevier applied science publisher's ltd
6. Crawford RJ, Paul DW, Sprevak D (1982) Solid phase compaction of polymeric powders: effects of compaction conditions on pressure and density variations. Polymer 23:123–128
7. Singh S, Sharma VS, Sachdeva A, Sinha SK (2013) Optimization and analysis of mechanical properties for selective laser sintered polyamide parts. Mater Manuf Process 28 (2):163–172
8. Sachdeva A, Singh S, Sharma VS (2013) Investigating surface roughness of parts produced by SLS process. Int J Adv Manuf Technol 64:1505–1516
9. Singh S, Sharma VS, Sachdeva A (2016) Progress in selective laser sintering using metallic powders: a review. Mater Sci Technol 32:760–772
10. Gibson I, Shi D (1997) Material properties and fabrication parameters in selective laser sintering process. Rapid Prototyping J 3:129–136
11. Williams JD, Deckard CR (1998) Advances in modeling the effects of selected parameters on the SLS process. Rapid Prototyping J 4:90–100
12. Ho HCH, Gibson I, Cheung WL (1999) Effects of energy density on morphology and properties of selective laser sintered polycarbonate. J Mater Process Technol 89–90:204–210
13. Tontowi AE, Childs THC (2001) Density prediction of crystalline polymer sintered parts at various powder bed temperatures. Rapid Prototyping J 7:180–184
14. Shi Y, Li Z, Sun H, Huang S, Zeng F (2004) Effect of the properties of the polymer materials on the quality of selective laser sintering parts. Proc Instn Mech Engrs Part L: J Mater Des Appl 218:247–252
15. Bugeda G, Cervera M, Lombera G (1999) Numerical prediction of temperature and density distributions in selective laser sintering processes. Rapid Prototyping J 5:21–26
16. Vijayaraghavan V, Garg A, Wong CH, Tai K, Regalla SP, Tsai MC (2016) Density characteristics of laser-sintered three-dimensional printing parts investigated by using an integrated finite element analysis–based evolutionary algorithm approach. Proc IMechE Part B: J Eng Manuf 230(1):100–110
17. Wudy K, Drummer D (2016) Aging behavior of polyamide 12: interrelation between bulk characteristics and part properties. Solid Freeform Fabrication Symposium—an Additive Manufacturing Conference 770–781
18. Spierings AB, Schneider M (2011) Comparison of density measurement techniques for additive manufactured metallic parts. Rapid Prototyping J 17:380–386
19. Gong H, Rafi K, Gu H, Starr T, Stucker B (2014) Analysis of defect generation in Ti-6Al-4V parts made using powder bed

fusion additive manufacturing processes. Additive Manuf 1–4: 87–98
20. Montgomery DC (2013) Design and analysis of experiments. John Wiley, Hoboken
21. Myers RH, Montgomery DC, Anderson CM (2008) Response surface methodology: process and product optimization using designed experiments. Wiley, New York
22. Frost J (2014) How to interpret a regression model with low R-squared and low P values. http://blog.minitab.com/blog/adventures-in-statistics-2/how-to-interpret-a-regression-model-with-low-rsquared-and-low-p-values. Accessed 24 Mar 2017